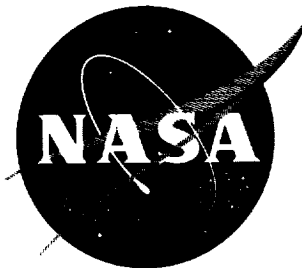~~CONFIDENTIAL~~

NASA TM X-726

NASA TM X-726

TECHNICAL MEMORANDUM

X-726

LATERAL-DIRECTIONAL CONTROL CHARACTERISTICS OF THE

X-15 AIRPLANE

By Commander Forrest S. Petersen, USN,
Herman A. Rediess, and Joseph Weil

Flight Research Center
Edwards, Calif.

DECLASSIFIED BY AUTHORITY OF NASA
CLASSIFICATION CHANGE NOTICES NO. 3
DATED 4-21-65 ITEM NO. 14

N65-23924

(ACCESSION NUMBER)

26
(PAGES)

(NASA CR OR TMX OR AD NUMBER)

(THRU)

/
(CODE)

02
(CATEGORY)

FACILITY FORM 602

GPO PRICE $ _____

OTS PRICE(S) $ _____

Hard copy (HC) $2.10 _____

Microfiche (MF) ____ .50 ____

NATIONAL AERONAUTICS AND SPACE ADMINISTRATION

TECHNICAL MEMORANDUM X-726

LATERAL-DIRECTIONAL CONTROL CHARACTERISTICS OF THE X-15 AIRPLANE* **

By Forrest S. Petersen, Herman A. Rediess, and Joseph Weil

SUMMARY

The deterioration of lateral-directional controllability with roll damper off and the pilot performing a lateral-control task is discussed. The problem area was defined by fixed-base and airborne simulators and verified by closed-loop analysis in which a human transfer function represents the pilot. A parameter which predicts the problem area for the X-15 airplane is developed. The means considered to alleviate the control problem in the X-15 airplane are also discussed.

INTRODUCTION   USE CARD IN BACK

As indicated in reference 1, a primary area of concern has been the lateral-directional dynamic instability with roll damper off. This condition corresponds to the potential emergency situation created by a stability-augmentation-system failure, since the X-15 airplane is intended to perform all its missions with the stability-augmentation system in operation.

Considerable effort has been expended in the investigation of the control problem which might follow a roll-damper failure. These investigations have utilized both fixed and airborne simulators, closed-loop theoretical analysis, and actual flight tests of the X-15 airplane. This paper reviews the results of these efforts as well as the action considered to alleviate the problem.

CONFIDENTIAL

SYMBOLS

b	wing span, ft
C_2	cycles to double amplitude
$C_{1/2}$	cycles to one-half amplitude
c_1, c_2, c_3	constants of a general third-order equation
C_l	$\dfrac{\text{Rolling moment}}{qSb}$
C_n	$\dfrac{\text{Yawing moment}}{qSb}$
$C_{l_\beta} = \dfrac{\partial C_l}{\partial \beta}$	
$C_{n_\beta} = \dfrac{\partial C_n}{\partial \beta}$	
I_X	moment of inertia about principal X-axis, slug-ft^2
I_Z	moment of inertia about principal Z-axis, slug-ft^2
K_P	pilot gain
$K_P{}' = K_P L_{\delta_a}$	
L	$\dfrac{\text{Rolling moment}}{I_X}$, per sec^2
$L_p = \dfrac{\partial L}{\partial p}$	
$L_\beta = \dfrac{\partial L}{\partial \beta}$	

$$L_{\delta_a} = \frac{\partial L}{\partial \delta_a}$$

M	Mach number
m	mass, slugs
N	$\dfrac{\text{Yawing moment}}{I_Z}$, per $\sec^2$

$$N_r = \frac{\partial N}{\partial r}$$

$$N_\beta = \frac{\partial N}{\partial \beta}$$

$$N_{\delta_a} = \frac{\partial N}{\partial \delta_a}$$

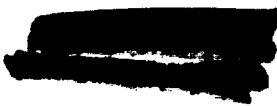|	
p	roll rate, deg/sec or radians/sec
q	dynamic pressure, lb/sq ft
r	yaw rate, radians/sec
S	wing area, sq ft
s	Laplace transform variable
s_i	roots of transfer function (i = 1,2,3...)
V	forward velocity, ft/sec
Y	$\dfrac{\text{Side force}}{mV}$, per sec

$$Y_\beta = \frac{\partial Y}{\partial \beta}$$

α	angle of attack, deg or radians

α_0 trim angle of attack of principal axis, radians

β angle of sideslip, deg or radians

δ_a aileron deflection, deg or radians

ζ_φ damping ratio of the numerator of the airplane transfer
        function in roll

ζ_ψ damping ratio of short-period Dutch roll mode

τ_1 pilot time constant, sec

τ_φ time constant in roll, sec

φ bank angle, deg or radians

θ general pole angle or zero angle

θ_i specific pole angle or zero angle $(i = 1,2,3...)$

ω_{n_φ} undamped natural frequency of the numerator of the airplane
        transfer function in roll, radians/sec

ω_{n_ψ} undamped natural frequency of short-period Dutch roll mode,
        radians/sec

Subscripts:

e   error

P   pilot

ref   reference

A dot over a symbol indicates the derivative of the quantity with respect to time.

GENERAL DISCUSSION

It became apparent early in six-degree-of-freedom simulations of reentries from altitude missions with the roll damper off that uncontrollable combinations of Mach number and angle of attack were frequently encountered. Stick-fixed stability analysis had not indicated that these uncontrollable conditions would be encountered. Figure 1 shows the uncontrollable area with the roll damper off in terms of angle of attack

plotted against Mach number as determined from extensive fixed-base simulator work. The criteria used in defining the uncontrollable area was actual loss of control. As a result, no fine line of demarcation between controllable and uncontrollable is implied or shown. The lighter shaded area indicates that the pilot was able to fly for longer periods before loss of control occurred. In the darker shaded areas loss of control is very rapid. Since the airplane is uncontrollable in the shaded area, no data with the stability-augmentation system of the X-15 airplane off were anticipated in this area. However, by using T-33 and F-100C variable-stability airplanes as in-flight simulators, several points within the area have been extensively evaluated.

To obtain flight verification in the X-15 airplane, pilots were instructed on several flights to explore the fringes of the predicted uncontrollable region. Figure 2 shows the flight conditions on one such flight in relation to the uncontrollable area. Figure 3 shows the airplane motions which occurred along this flight path. At the beginning of the flight path and time history, the airplane was at an angle of attack of approximately $7°$ and the pilot turned the roll and yaw dampers off. Lateral motions immediately began to build up, so he reduced the angle of attack. The motions subsided and angle of attack was again increased. Again the motions began to build up, and the angle of attack had to be reduced. Although the pilot was holding on to the center stick, he was not consciously making any lateral-control inputs. However, there were lateral-control inputs, as shown in the figure.

Figure 4 shows the destabilizing effect of two types of pilot inputs in a time history for an F-100C variable-stability airplane. In the first portion of the time history, the pilot attempted to hold the stick fixed as in the previous time history. As in the time history with the X-15 airplane (fig. 3), there is a definite lateral-control input and a resultant divergent oscillation. During the center portion of the time history, the pilot released the stick and the oscillations were obviously damped. In the last portion the pilot attempted to control bank angle in a conventional manner; that is, lateral-control inputs are generally proportional to bank angle and in a direction to keep bank-angle excursions low. The similarity of the inadvertent lateral inputs and divergent oscillation in the first part of the time history to those in the last portion should be noted.

ANALYSIS OF THE LATERAL-CONTROL PROBLEM

Analytic closed-loop investigations of the X-15 (see fig. 5) indicate that the uncontrollable region can be predicted. The following transfer function, developed in reference 2 and used in reference 3,

closely approximates the control inputs of a pilot applying lateral
control proportional to bank angle plus a lead:

$$\frac{\delta_a(s)}{\varphi(s)} = K_p(1 + 0.57s) \qquad (1)$$

No directional control is considered during reentry conditions of rapidly
changing dynamic pressure, angle of attack, and Mach number. The rolling
moments resulting from directional control vary greatly in magnitude and
even change sign. This precludes effective use of directional control
during reentry.

It is shown in reference 3 that the characteristic equation of the
pilot-airplane system (see fig. 5) is obtained by combining the pilot
transfer function with the transfer function for roll response to lateral-
control inputs as follows:

$$\frac{K_p L_{\delta_a}(1 + 0.57s)\left[s^2 + \left(-N_r - Y_\beta\right)s + N_\beta - L_\beta\dfrac{N_{\delta_a}}{L_{\delta_a}} + N_r Y_\beta\right]}{s^4 + \left(-Y_\beta - N_r - L_p\right)s^3 + \left(N_\beta - \alpha_o L_\beta + Y_\beta N_r + Y_\beta L_p + N_r L_p\right)s^2 + \left(-L_p N_\beta + \alpha_o L_\beta N_r - Y_\beta N_r L_p\right)s} = \text{-}1 \quad (2)$$

which is of the form,

$$\frac{K_p'(1 + 0.57s)\left(s^2 + 2\zeta_\varphi \omega_{n_\varphi}s + \omega_{n_\varphi}^2\right)}{s\left(s + \dfrac{1}{\tau_\varphi}\right)\left(s^2 + 2\zeta_\psi \omega_{n_\psi}s + \omega_{n_\psi}^2\right)} = -1 \qquad (3)$$

The closed-loop stability of the system is then determined by solving
for the roots of equation (2). In figure 6 the neutral stability of
the X-15 airplane defined by the roots of equation (2) is compared with
the uncontrollable envelope. The area within this boundary is predicted
to be unstable with the pilot in the loop and is in reasonable correlation
with the simulator results.

An analysis of this general type of control problem has been per-
formed in reference 4 by using root-locus methods (see ref. 5). The
specific control problem of the X-15 airplane has been analyzed in
reference 3 using a root-locus approach slightly different from that

used in reference 4. A portion of the analysis of reference 3 is briefly repeated herein to describe a useful parameter which relates the severity of the control problem to familiar aerodynamic derivatives and provides a better understanding of the problem.

Figures 7(a) and 7(b) present typical root loci of the pilot-airplane transfer function in roll (the left-hand side of equation (3)) for controllable and uncontrollable situations, respectively. The complex poles represent the stick-fixed Dutch roll stability. The line drawn from the complex pole to the complex zero (locus of the roots) represents the changing stability of the pilot-airplane system with increasing pilot gain. In figure 7(a), the pole is above the zero and, therefore, the locus closes in the stabilizing direction; however, when the zero is above the pole the locus closes in the destabilizing direction and may cross over into the unstable right half of the plane. The difference between the distances of the zero and pole from the origin $\omega_{n_\varphi} - \omega_{n_\psi}$ is suggested as an indication of the possibility of an uncontrollable condition. For aircraft with low lateral-directional damping, such as the X-15, this difference can be closely approximated by the following equation:

$$\omega_{n_\varphi} - \omega_{n_\psi} \approx \frac{L_\beta \left(\alpha_o - \dfrac{N_{\delta_a}}{L_{\delta_a}} \right)}{2\omega_{n_\psi}} \tag{4}$$

When $\omega_{n_\varphi} - \omega_{n_\psi}$ is negative, as in figure 7(a), this control problem does not exist; however, other types of lateral-control problems may or may not exist. If it is positive, as in figure 7(b), this type of control problem will exist if the value of $\omega_{n_\varphi} - \omega_{n_\psi}$ is sufficiently large and the basic airplane damping is low enough.

It is shown in the appendix that the maximum decrement of damping which the pilot might provide when $\omega_{n_\varphi} - \omega_{n_\psi}$ is positive is approximately proportional to $\omega_{n_\varphi} - \omega_{n_\psi}$ for the X-15 airplane. An increasing positive value of this parameter represents an increasing decrement in the damping of the closed-loop pilot-airplane system. A cumbersome but more exact expression is given in the appendix (eq. (A9)).

In references 6 and 7 it was shown that the X-15 airplane above a Mach number of 2.3 has undesirable positive values of C_{l_β}. The aileron cross-coupling term $\dfrac{N_{\delta_a}}{L_{\delta_a}}$ of equation (4) is a small quantity; therefore,

the positive product of L_β and α_o predominates. Figure 8 shows that, whereas in the angle-of-attack range from $5°$ to $15°$, the X-15 airplane is predicted to be nearly neutrally stable, the addition of the pilot in the loop deteriorates the stability markedly so that an oscillation doubles the amplitude in one-half cycle at $\alpha = 12°$. The pilot-airplane curve was calculated by using equation (A9).

Simulator studies have shown that this controllability parameter (eq. (4)) correlates well with pilot opinion for the X-15 airplane. Figure 9 shows the variation of pilot ratings with the values of $\omega_{n_\varphi} - \omega_{n_\psi}$. The conditions for the X-15 airplane were selected and flown in five degrees of freedom which gave the values of $\omega_{n_\varphi} - \omega_{n_\psi}$ as indicated in the figure. It is seen that there is a definite deterioration of pilot opinion with increasing positive values of the parameter. This parameter is not presented as a general criterion for all lateral-directional control problems but, rather, as a means of explaining the type of controllability problem which is discussed in this paper. It can be used for indicating the possibility of the specific type of control problem existing in other aircraft if the assumptions used in its derivation are compatible with the particular aircraft.

POSSIBLE METHODS OF ALLEVIATING THE LATERAL-CONTROL PROBLEM

As soon as it was suspected that a large portion of the flight envelope for the X-15 airplane was uncontrollable with lateral-stability augmentation off, investigations were initiated to find ways of alleviating the problem. The first method tried, because it would have been the easiest to implement, was pilot-display quickening. Sideslip and bank-angle presentations were quickened by including yaw rate and roll rate, respectively. Various quickening gains were used in the investigation on the fixed-base simulator, but no combination which significantly improved the pilot's ability to handle the instability was found.

The use of ailerons to control sideslip angle for certain types of airplane instabilities has been investigated independently by personnel of North American Aviation, Inc., and the NASA Flight Research Center, Edwards, Calif. Figure 10 shows a time history illustrating the use of a nonconventional control technique which evolved from these investigations and showed considerable promise on a fixed-base simulator. The first part of the time history shows, again, the destabilizing effect of conventional lateral-control inputs. In the last part of the time history, a method referred to as the $\dot\beta$ technique was used. It consists of sharp, lateral-control inputs to the left, as the nose swings left through zero sideslip, and vice versa. At this time $\dot\beta$ is maximum.

The pilot flies hands-off except when making the lateral pulses. This is desirable in flight because of the instability induced by the inadvertent inputs associated with merely holding on to the center stick.

Figure 11 shows a comparison of the effectiveness of the $\dot{\beta}$ technique on fixed-base and airborne simulators with the center stick. The solid line represents pilot opinion of using conventional lateral-control techniques on either simulator. The short dashed line represents pilot opinion of using the $\dot{\beta}$ technique on the fixed-base simulator. The long dashed lines represent pilot opinion of the $\dot{\beta}$ technique in the F-100C airplane. Fixed-base ratings indicated considerable improvement with this technique. However, experience in the F-100C indicated that the improvement achieved in terms of pilot opinion of the handling qualities was greatly reduced as the roll-damper gain was reduced to zero. Use of the side-located controller in the X-15 airplane has provided some relief from the destabilizing effect of inadvertent inputs present with the center stick and makes the $\dot{\beta}$ technique more effective. Figure 12 shows the uncontrollable area and indicates regions in which pilots have successfully flown the X-15 airplane with the side-located controller by using the $\dot{\beta}$ technique with roll damper intentionally off. Pilots feel that they were able to fly sufficiently well in the shaded area of figure 12 to permit a successful reentry from a flight to an altitude of 250,000 feet. Previous experience with the center stick indicated the controllable angle of attack to be considerably lower. All X-15 pilots are well versed in the use of the $\dot{\beta}$ technique. Its usefulness may, however, be even less than was indicated when the pilot has the task of maintaining bank-angle excursions from zero to small values as he does in a reentry. Furthermore, a lateral input in the wrong direction, which is a conceivable mistake with other problems clamoring for the pilot's attention, could be disastrous.

As was indicated in reference 6, recent efforts have been directed toward the evaluation of the handling qualities of the X-15 airplane with the lower rudder off. Figure 13 shows the variation of C_{l_β} and C_{n_β} with Mach number at an angle of attack of 12° with the lower rudder on and off. The upper portion of the figure shows that desirable negative values of C_{l_β} are realized throughout the Mach number range at this angle of attack with the lower rudder off as contrasted with undesirable positive values of C_{l_β} with the lower rudder on at all Mach numbers above about 2.3. This favorable value of C_{l_β} is not realized without a reduction in C_{n_β} as is shown in the bottom half of figure 13. However, as was pointed out in reference 6 the Dutch roll stability is increased by negative values of C_{l_β}.

Figure 14 shows the uncontrollable areas in terms of angle of attack and Mach number as predicted by fixed-base simulators with lower rudder on. Figure 15 shows the predicted uncontrollable area based on closed-loop analysis and fixed-base simulator studies for the lower rudder off. The solid lines in figures 14 and 15 indicate the conditions followed just prior to and during reentry on a typical altitude mission. With the lower rudder on, a considerable portion of the reentry from an altitude mission is within the uncontrollable region as shown in figure 14. Figure 15 shows that a reentry conducted with the lower rudder off does not penetrate the predicted uncontrollable region. The flight conditions on the X-15 flight with the lower rudder off are shown as dashed lines in figure 15. In the limited area explored on this flight, the flying qualities were as good as or better than those predicted by the fixed-base and airborne simulators. However, as predicted, the flying qualities at low angles of attack were worse with the lower rudder off than with the lower rudder on. Additional flights are being planned in the X-15 airplane to evaluate further the handling qualities with lower rudder off. If these tests continue to indicate favorable trends and no severe problem areas are uncovered, the configuration with the lower rudder off may offer undeniable advantages for the high-angle-of-attack, reentry portion of an altitude mission.

Since control characteristics are reasonably good with the stability-augmentation system on, one way in which the potential problem area can be improved is by reducing the possibility of a critical augmentation failure. This is to be accomplished by dualization of certain components in the augmentation system.

<div align="center">H
2
6
9</div>

CONCLUDING REMARKS

A serious lateral-directional control problem with the X-15 airplane with the lower rudder on and the roll damper off at high angles of attack has been uncovered. The problem is caused primarily by negative dihedral effect and was not revealed until the inputs of the pilot were used with airplane stability to determine closed-loop stability. The use of a transfer function which represents the inputs of a pilot performing a lateral-control task permits calculation of the degree of pilot-airplane instability. Although special control techniques have not completely alleviated the problem, they have provided sufficient improvement when utilizing the side stick to allow flight in the fringes of the uncontrollable region. Removal of the lower rudder appears promising as a means of alleviating the lateral-directional instability at high angles of attack associated with a roll-damper failure. Finally, additional
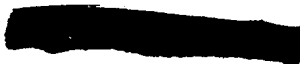
reliability will be obtained by dualization of certain components in the stability-augmentation system.

Flight Research Center
National Aeronautics and Space Administration
Edwards, Calif., November 20, 1961.

H
2
6
9

APPENDIX

DECREMENT IN DAMPING DUE TO THE PILOT

The controllability parameter developed in reference 2

$$\omega_{n_\varphi} - \omega_{n_\psi} \approx \frac{L_\beta \left(\alpha_o - \dfrac{N_{\delta_a}}{L_{\delta_a}} \right)}{2\omega_{n_\psi}} \tag{A1}$$

will be used in the derivation of an expression for the maximum decrement in damping which a pilot might provide while performing a lateral-control task. This derivation assumes the following:

(1) The damping in roll and the Dutch roll damping are low.

(2) $\omega_{n_\psi} \gg \omega_{n_\varphi} - \omega_{n_\psi}$

(3) The pilot-time constant τ_1 is less than an order of magnitude different from the roll-mode time constant.

These assumptions are compatible with the characteristics of the X-15 airplane and the derivation of equation (A1). First, it is necessary to establish that the root locus (see ref. 5) from the complex pole to the complex zero is approximately a semicircle, as shown in the following sketch, under these assumptions:
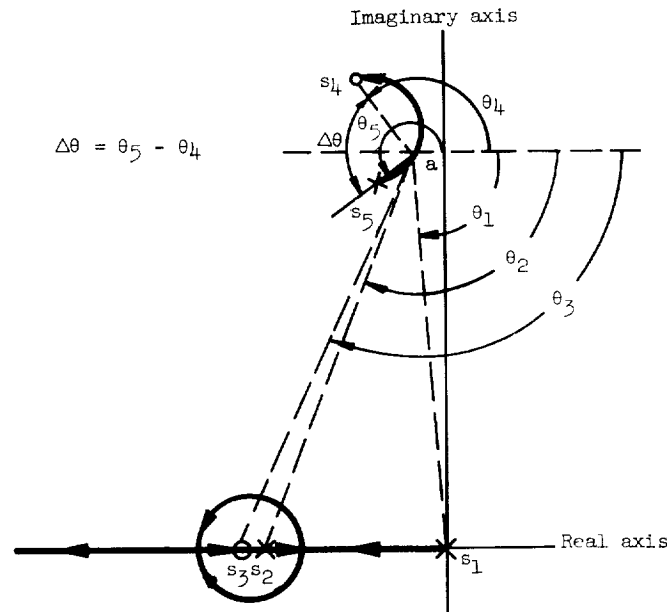
By definition of root locus at some point a on the locus of the preceding sketch,

$$\Sigma\theta = 180^\circ$$

also

$$\Sigma\theta = \Sigma \text{ Pole angles} - \Sigma \text{ Zero angles}$$

that is,

$$\Sigma\theta = \theta_1 + \theta_2 + \theta_5 - \theta_4 - \theta_3 = 180^\circ$$

Because of assumption 1,

$$\theta_1 \approx 90^\circ$$

Because of assumption 3,

$$\theta_2 \approx \theta_3$$

Therefore,

$$\Sigma\theta \approx 90^\circ + \theta_5 - \theta_4 \approx 180^\circ$$

or

$$\Delta\theta = \theta_5 - \theta_4 \approx 90^\circ$$

therefore the locus is approximately a semicircle. Note that $\theta_1 \approx 90^\circ$ and $\theta_2 \approx \theta_3$ both provide conservative answers because deviations from these approximations for the X-15 airplane are in the direction to increase $\Delta\theta$; thus, the actual stability will be greater than the semicircle approximation.

The maximum pilot-damping decrement $\left[\zeta\omega_n\right]_P$ is derived with the aid of the following sketch:
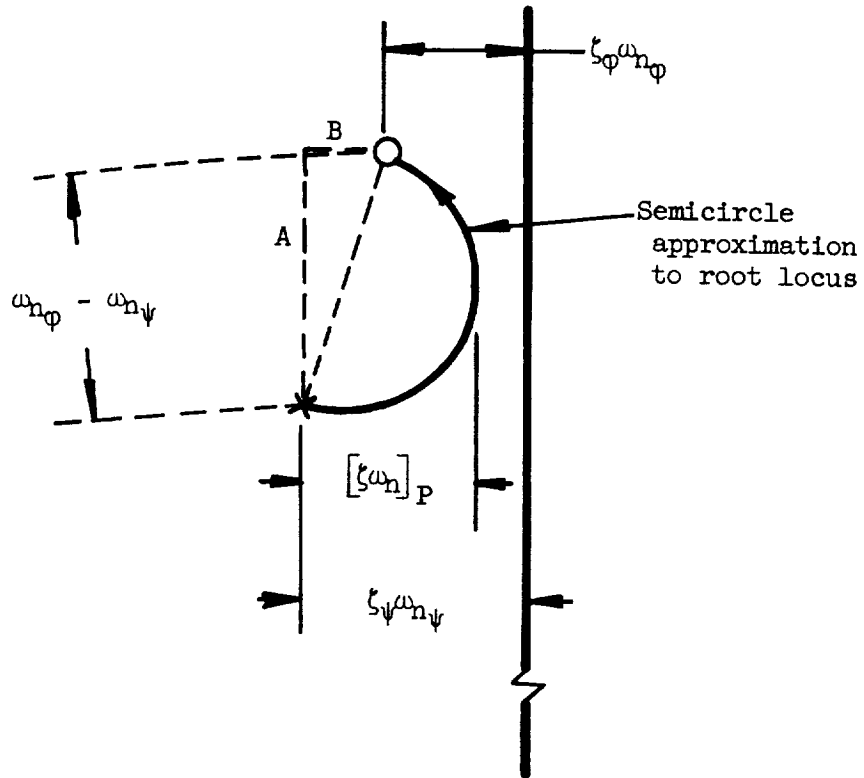
H-269

Simple geometric relations show that

$$\left[\zeta\omega_n\right]_P = \frac{1}{2}\left(B + \sqrt{B^2 + A^2}\right) \tag{A2}$$

where

$$A \approx \omega_{n_\varphi} - \omega_{n_\psi} \tag{A3}$$

and

$$B = \zeta_\psi\omega_{n_\psi} - \zeta_\varphi\omega_{n_\varphi} \tag{A4}$$

By comparing equations (2) and (3) in the discussion it can be seen that

$$\zeta_\varphi \omega_{n_\varphi} = 1/2\left(-N_r - Y_\beta\right) \qquad (A5)$$

In order to obtain an expression for $\zeta_\psi \omega_{n_\psi}$, the third-order equation which is reduced from the denominator of equation (2) must be solved. A good approximate solution to a third-order equation of the form,

$$s^3 + c_1 s^2 + c_2 s + c_3 = 0 \qquad (A6)$$

when $c_3 \ll c_2$, as for the X-15 airplane, is to assume a real root to be

$$s_1 = -\frac{c_3}{c_2}$$

and then solve by synthetic division. This method yields the following approximate expressions when small terms are neglected:

$$\zeta_\psi \omega_{n_\psi} \approx \frac{1}{2}\left[\left(-N_r - Y_\beta\right) + \left(L_p - N_r\right)\left(\frac{\alpha_o L_\beta}{N_\beta - \alpha_o L_\beta}\right)\right] \qquad (A7)$$

and

$$\omega_{n_\psi}^2 \approx N_\beta - \alpha_o L_\beta \qquad (A8)$$

Substituting equations (A5), (A7), and (A8) into equation (A2) and reducing to simplest form leads to the following expression for the maximum damping decrement the pilot might provide:

$$\left[\zeta\omega_n\right]_P \approx \frac{1}{2}\left\{\frac{\alpha_o L_\beta\left(L_p - N_r\right)}{2\omega_{n_\psi}^2} + \sqrt{\left[\frac{\alpha_o L_\beta\left(L_p - N_r\right)}{2\omega_{n_\psi}^2}\right]^2 + \left[\frac{L_\beta\left(\alpha_o - \frac{N_{\delta_a}}{L_{\delta_a}}\right)}{2\omega_{n_\psi}}\right]^2}\right\} \qquad (A9)$$

For the X-15 airplane at moderate to high angles of attack, the term

$$\frac{\alpha_o L_\beta \left(L_p - N_r\right)}{2\omega_{n_\psi}^2}$$

is generally smaller than the remaining term and the following can be used for a first approximation:

$$\left[\zeta\omega_n\right]_P \approx \frac{L_\beta\left(\alpha_o - \dfrac{N_{\delta_a}}{L_{\delta_a}}\right)}{4\omega_{n_\psi}} = \frac{\omega_{n_\varphi} - \omega_{n_\psi}}{2} \qquad (A10)$$

H
2
6
9
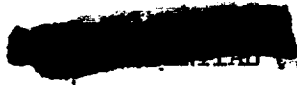
REFERENCES

1. White, Robert M., Robinson, Glenn H., and Matranga, Gene J.: Résumé of Handling Qualities of the X-15 Airplane. NASA TM X-715, 1962.

2. Taylor, Lawrence W., Jr., and Day, Richard E.: Flight Controllability Limits and Related Human Transfer Functions as Determined From Simulator and Flight Tests. NASA TN D-746, 1961.

3. Taylor, Lawrence W., Jr.: Analysis of a Pilot-Airplane Lateral Instability Experienced With the X-15 Airplane. NASA TN D-1059, 1961.

4. Ashkenas, Irving L., and McRuer, Duane T.: The Determination of Lateral Handling Quality Requirements From Airframe - Human Pilot Studies. WADC Tech. Rep. 59-135, ASTIA Doc. No. AD 212 152, U. S. Air Force, June 1959.

5. Evans, Walter R.: Control-System Dynamics. McGraw-Hill Book Co., Inc., New York, 1954.

6. Walker, Harold J., and Wolowicz, Chester H.: Stability and Control Derivative Characteristics of the X-15 Airplane. NASA TM X-714, 1962.

7. Yancey, Roxanah B., Rediess, Herman A., and Robinson, Glenn H.: Aerodynamic-Derivative Characteristics of the X-15 Research Airplane as Determined From Flight Tests for Mach Numbers From 0.6 to 3.4. NASA TN D-1060, 1962.

18

LATERAL—DIRECTIONAL PROBLEM AREA
ROLL DAMPER OFF
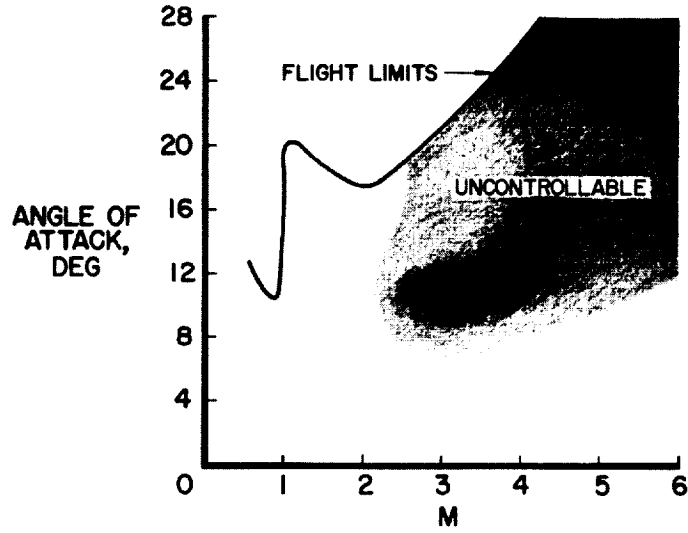
Figure 1

INITIAL FLIGHT STUDY
ROLL DAMPER OFF
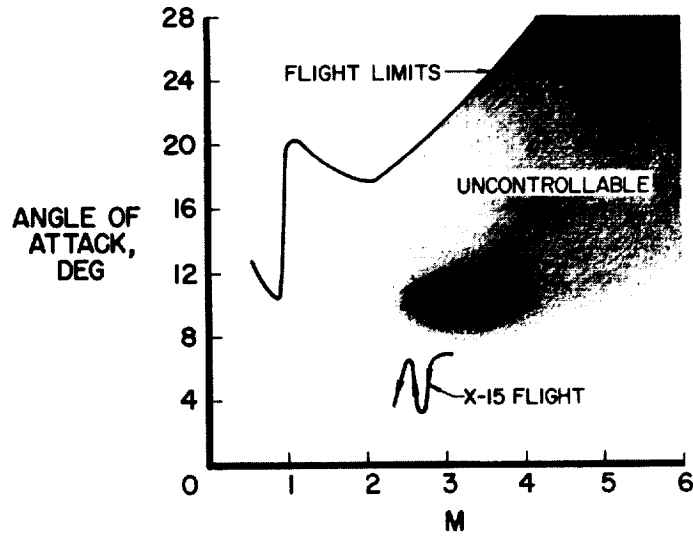
Figure 2
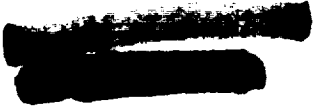
ANGLE-OF-ATTACK EFFECT ON X-15 CONTROLLABILITY
X-15 FLIGHT -ROLL DAMPER OFF
CENTER STICK
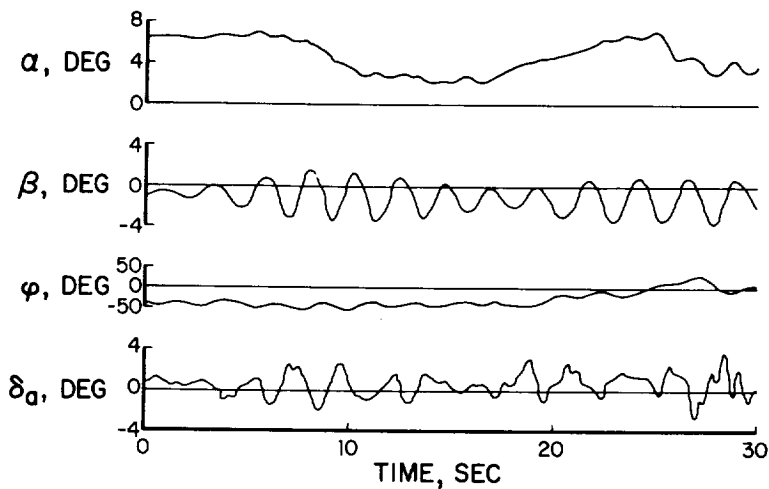
Figure 3

EFFECT OF PILOT ON CONTROLLABILITY
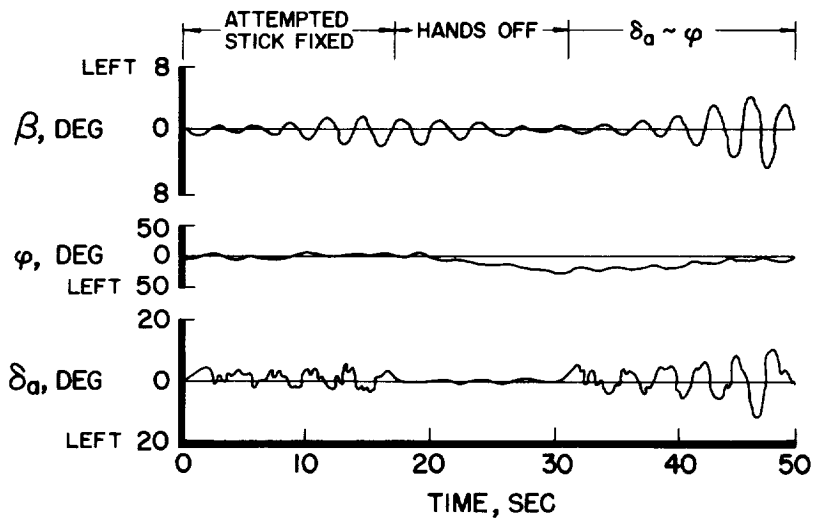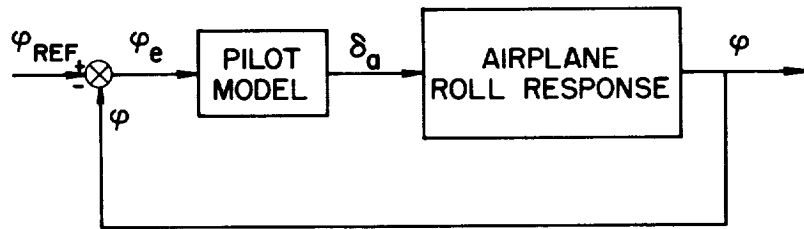### F-100C VARIABLE-STABILITY AIRPLANE

Figure 4

PILOT–AIRPLANE CLOSED-LOOP SYSTEM
FOR LATERAL CONTROL

PILOT MODEL $\quad \dfrac{\delta_a(s)}{\varphi_e(s)} = K_p(1+\tau_1 s)$

$$\text{AIRPLANE} \atop \text{ROLL RESPONSE} \quad \frac{\varphi(s)}{\delta_a(s)} = \frac{L_{\delta_a}\left(s^2 + 2\zeta_\varphi\,\omega_{n_\varphi}s + \omega_{n_\varphi}^2\right)}{s\left(s + \frac{1}{\tau_\varphi}\right)\left(s^2 + 2\zeta_\psi\,\omega_{n_\psi}s + \omega_{n_\psi}^2\right)}$$

Figure 5

COMPARISON OF CALCULATED AND SIMULATED
CONTROLLABILITY BOUNDARIES
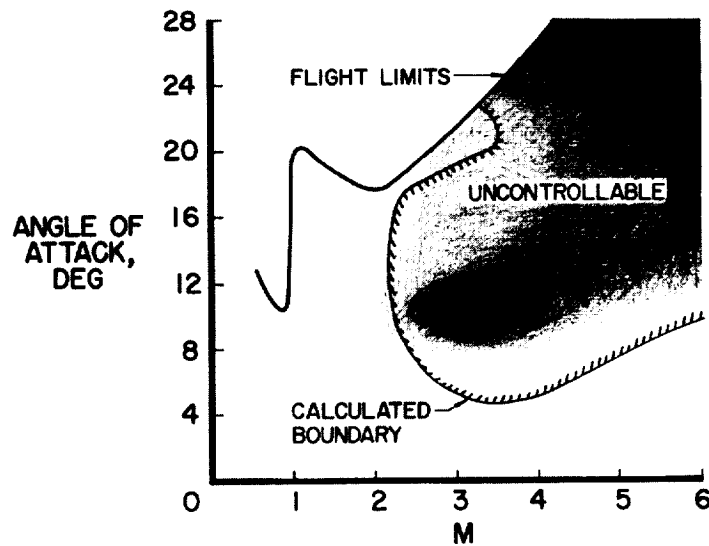
Figure 6

H-269

ROOT-LOCUS EXPLANATION OF CONTROL PROBLEM

o ZEROS
× POLES
□ COMPLEX ROOT FOR A
   SPECIFIC PILOT GAIN

$$\omega_{n_\varphi} - \omega_{n_\psi} \approx \frac{L_\beta \left(\alpha_0 - \dfrac{N_{\delta_a}}{L_{\delta_a}} \right)}{2 \, \omega_{n_\psi}}$$

IMAGINARY AXIS

$\zeta = \sin \theta$

θ

ω_n

REAL AXIS

(a) CONTROLLABLE

IMAGINARY AXIS

ω_{n_φ}

ω_{n_ψ}

REAL AXIS

(b) UNCONTROLLABLE
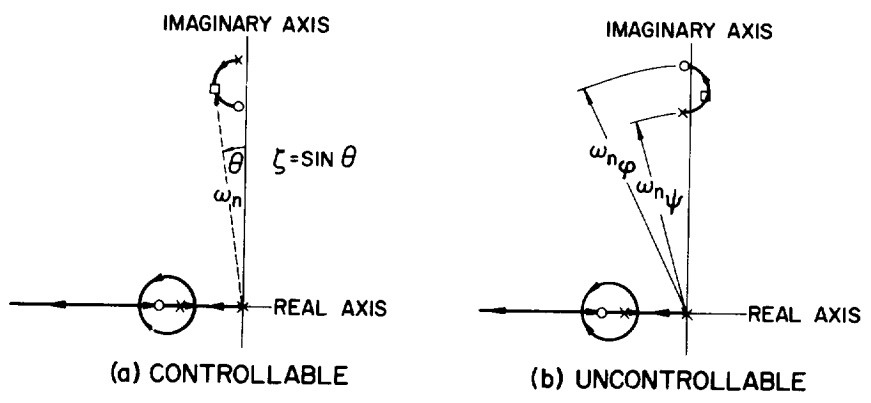
Figure 7

ANALYSIS OF THE PROBLEM
M=3.5, q=400 PSF

STABLE $\dfrac{1}{C_{1/2}}$

$\dfrac{1}{C_2}$

UNSTABLE

AIRPLANE

DAMPING
DECREMENT

AIRPLANE + PILOT

ANGLE OF ATTACK, DEG
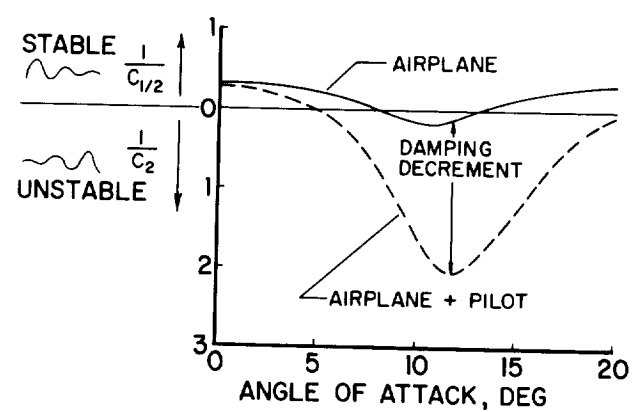
Figure 8

CORRELATION OF PILOT OPINION AND
CONTROLLABILITY PARAMETER
FIXED-BASE X-15 SIMULATOR
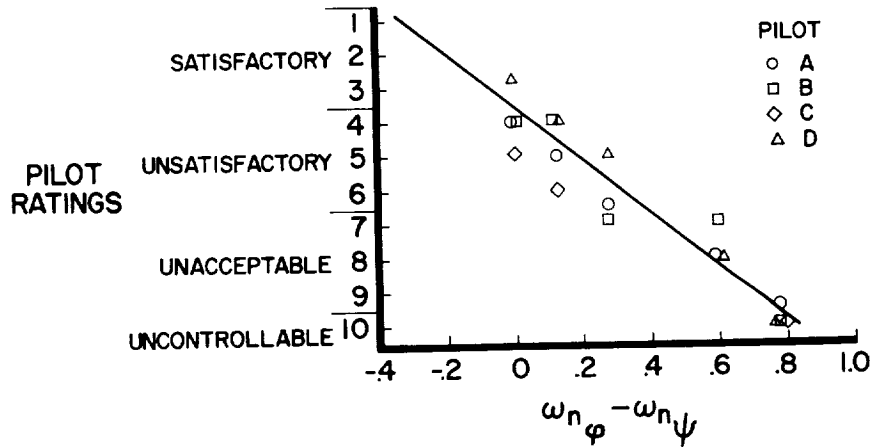
Figure 9

ILLUSTRATION OF $\dot{\beta}$ CONTROL TECHNIQUE
FIXED BASE X-15 SIMULATOR
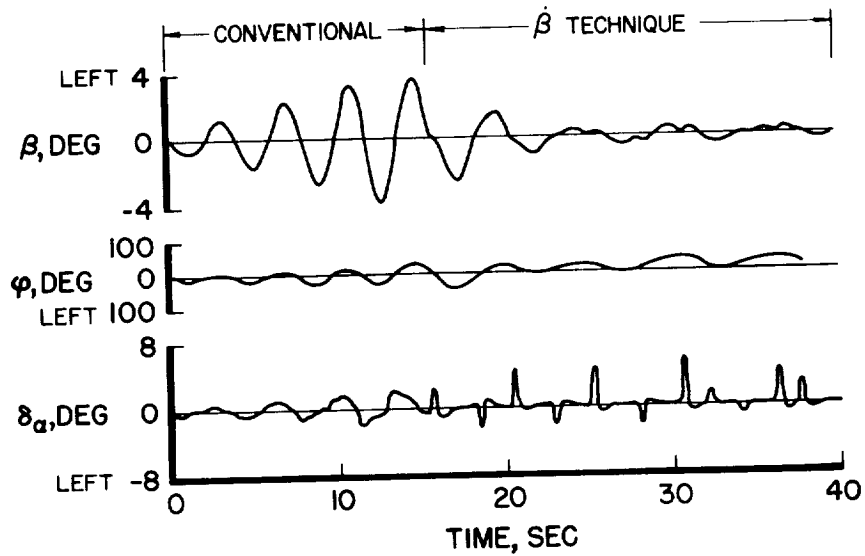
Figure 10

EFFECT OF MOTION CUES ON
$\dot{\beta}$ CONTROL TECHNIQUE
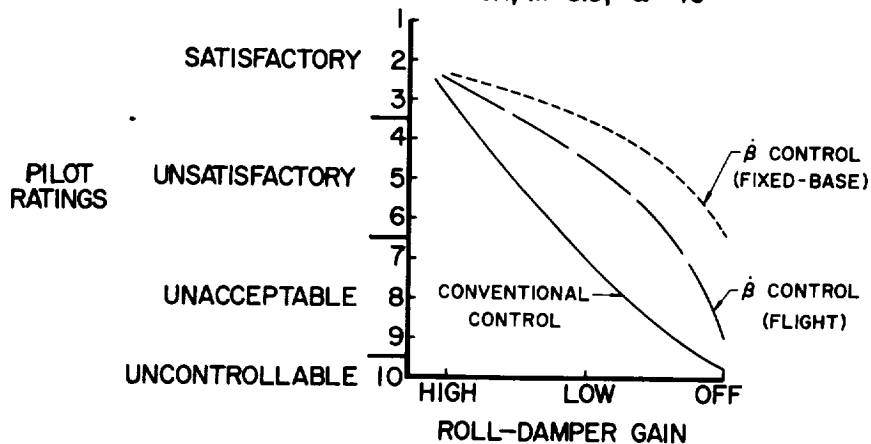### CENTER STICK, M=3.5, $\alpha = 10°$

Figure 11

X-15 FLIGHT STUDIES WITH SIDEARM
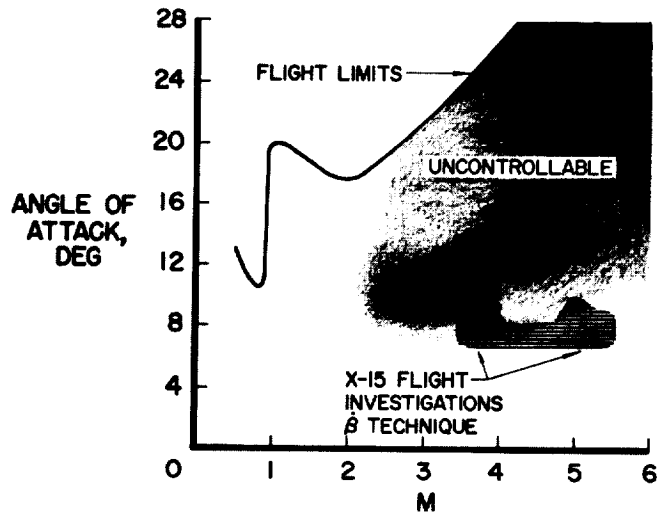## CONTROLLER
ROLL DAMPER OFF

Figure 12

24

EFFECT OF LOWER RUDDER ON DERIVATIVES
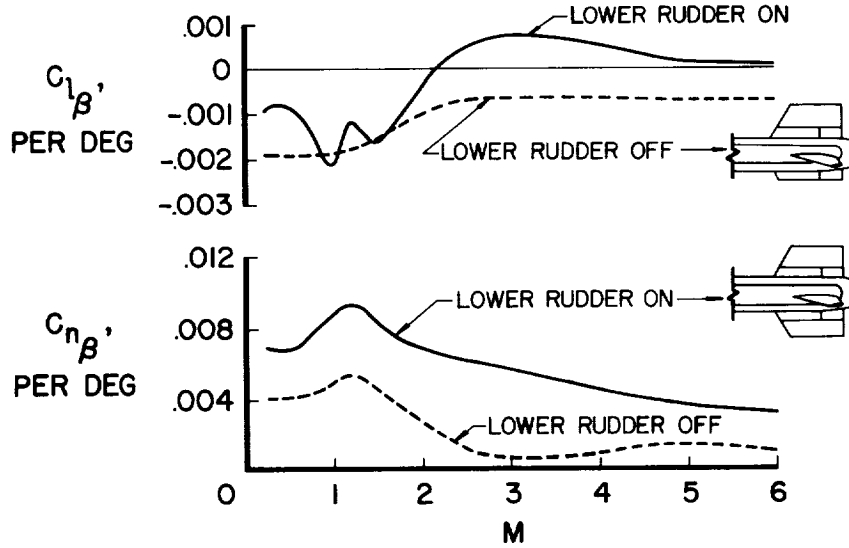### WIND-TUNNEL DATA, $\alpha = 12°$

Figure 13

RELATION OF REENTRY TO CONTROLLABILITY BOUNDARY
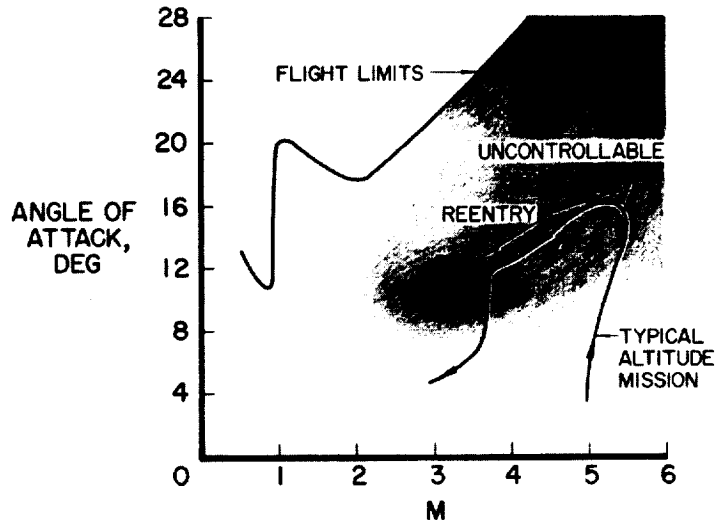### LOWER RUDDER ON — ROLL DAMPER OFF

Figure 14

RELATION OF REENTRY TO CONTROLLABILITY BOUNDARY
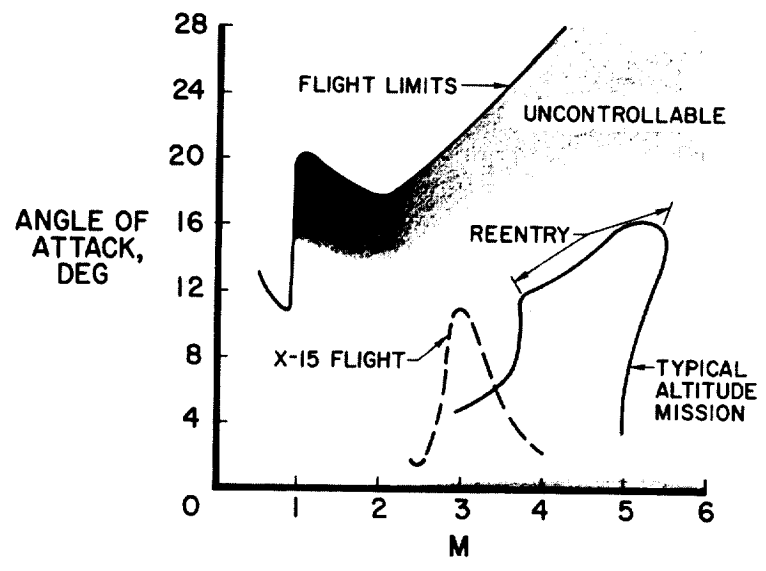### LOWER RUDDER OFF — ROLL DAMPER OFF

Figure 15